A first step towards the mapping of gas-phase CO2 in the headspace of champagne glasses

Anne-Laure Moriaux, Raphaël Vallon, Clara Cilindre, Frédéric Polak, Bertrand Parvitte, Gérard Liger-Belair, Virginie Zeninari

A first step towards the mapping of gas-phase CO_2 in the headspace of champagne glasses.

Anne-Laure MORIAUX, Raphaël VALLON, Clara CILINDRE, Frédéric POLAK, Bertrand PARVITTE, Gérard LIGER-BELAIR, Virginie ZENINARI*

Equipe Effervescence, Champagne et Applications, Groupe de Spectrométrie Moléculaire et Applications (GSMA), UMR CNRS 7331, Université de Reims Champagne-Ardenne, B.P.1039, 51687 Reims Cedex 2, France

Abstract

Key upgrades to a previously developed CO_2-Diode Laser Sensor (CO_2-DLS) were done to monitor as accurately as possible the level of gas-phase CO_2 in champagne glasses. The upgraded CO_2-DLS allows to access a wide range of CO_2 concentrations (10-100 %). An additional set of mirrors with two pairs of galvanometer scanners was developed in order to provide simultaneous measurements of gas-phase CO_2 concentrations in the whole glass headspace. During the five minutes after pouring, the CO_2-DLS unambiguously unveiled horizontal homogeneity in the glass headspace in terms of gas-phase CO_2 concentrations. Nevertheless, a strong vertical gradient of gas-phase CO_2 was highlighted, with ever increasing CO_2 concentrations ranging from approximately 15 % to 50 % while moving away from the glass edge to the champagne interface. This strong vertical gradient was found to persist during the five next minutes following the pouring process, but with ever decreasing CO_2 concentrations as time elapses.

Keywords: gas sensor, CO_2, diode laser spectrometry, Champagne, effervescence

*Virginie ZENINARI
Email address: virginie.zeninari@univ-reims.fr (Virginie ZENINARI)

Highlights

- Key upgrades to a CO_2 – diode laser sensor for enological applications are presented.
- Two off-axis parabolic mirrors with galvanometric mirrors are dedicated to the scanning.
- Monitoring gas-phase CO_2 in the headspace of a champagne glass was done, in space and time.
- Horizontal homogeneity and vertical stratification of gas-phase CO_2 above the champagne surface were highlighted.

Abbreviations

- CO_2 : carbon dioxide
- CO_2-DLS : CO_2-Diode Laser Sensor
- VOC : Volatile Organic Compound
- TDLAS : Tunable Diode Laser Absorption Spectrometer
- FP : Fabry-Pérot
- GM : Galvanometric mirrors
- D1 : Detector #1 ; D2 : Detector #2
- FPGA : Field-Programmable Gate Array
- FSIR : Full Scale Input Range
- DDS : Direct Digital Synthesizer
- INAO : Institut National des Appellations d'Origine or National Institute of Origin and Quality

1. Introduction

Nowadays, champagne has become the most renowned French sparkling wine, praised world-wide for the fineness of its effervescence. Champagne and sparkling wines elaborated through the same traditional method are under a high pressure of carbon dioxide (CO_2), as gas-phase CO_2 forms together with ethanol during a second in-bottle fermentation process promoted by adding yeasts and a certain amount of sugar in bottles hermetically sealed with a crown cap or a cork stopper [1, 2]. This second in-bottle fermentation process forced an amount equivalent to around 11-12 $g \cdot L^{-1}$ of CO_2 to progressively dissolve into the wine, according to the so-called Henry's law [1]. From a strictly chemical point of view, Champagne wines can thus be seen as multicomponent hydroalcoholic systems, supersaturated with dissolved CO_2, with a density close to unity, a surface tension and a viscosity about 50 % larger than that of pure water (mainly due to the presence of 12-13 % v/v ethanol) [1]. In sparkling beverages in general, and in champagne and sparkling wines in particular, the level of dissolved CO_2 found in the liquid phase is indeed a parameter of paramount importance since it is responsible for the visually appealing, and very much sought-after repetitive bubbling process (the so-called effervescence).

During Champagne or sparkling wine tasting, gas-phase CO_2 and volatile organic compounds (VOC) invade the headspace above glasses [1], thus progressively modifying the chemical space perceived by the consumer. Gas-phase CO_2 in excess can even cause a very unpleasant tingling sensation perturbing both ortho- and retronasal olfactory perception [3]. In recent years, both glass-shape and the CO_2 bubbling rates were found to play key roles concerning the rate at which dissolved CO_2 escapes from champagne, under standard tasting conditions [4–7]. Moreover, the temperature of champagne was also found to be a key parameter as concerns the losses of dissolved CO_2 from champagne glasses [8]. For all the aforementioned reasons, no wonder that the complex interplay between the level of dissolved CO_2 found in champagne, its temperature [8], the glass shape [4, 6, 7, 9], and the bubbling rate [5], finally impacts champagne tasting by modify-

ing the neuro-physico-chemical mechanisms responsible for aroma release and flavour perception. Following these recent highlights, monitoring as accurately as possible the level of gas-phase CO_2 above glasses is therefore a challenge of importance aimed at better understanding the close relationship between the release of CO_2 and a collection of various tasting parameters.

In many fields of research, gas-phase CO_2 must be accurately monitored, such as for example in the field of biology [10, 11], environmental studies [12, 13], or in medicine [14, 15]. In order to measure a molecule of interest in a non-invasive way, analytical methods must be used to separate, identify and quantify it. The use of sensors and the development of gas-phase CO_2 analysis methods in the food industry is widespread [16], particularly in the analysis of food packaging [17] and the brewing industry [18, 19]. For example, the RoboBEER [20], aimed at measuring the release of gas-phase CO_2 by a sensor (MG-811), is based on the principle of a solid electrolyte battery. However, this sensor requires calibration and heating time, and it covers a small range of gas-phase CO_2 concentrations, between 0.04 and 1 %. A standard microgas chromatography can also be used in order to measure gas-phase CO_2 [21, 22]. This method nevertheless requires a calibration and it shows a low temporal resolution between successive measurements. Gas-phase CO_2 can also be detected through a hyperspectral camera [23]. The system requires a light source, such as a laser diode, adapted to the wavelength of absorption of the gas of interest (CO_2). This method could allow the quantification of CO_2 in a wide concentration range (0 to 100 %) but also requires an upstream calibration. Finally, in the field of spectroscopy, the tunable diode laser absorption spectroscopy (TDLAS) is predominantly used and seems to be the best solution to monitor gas-phase CO_2 [24]. It allows the measurement of gas-phase CO_2 up to 100 % without requiring any calibration. Based on the TDLAS, CO_2 gas sensors have been developed for atmospheric applications [25, 26], power plant exhausts [27], combustion applications [28] and exhaled human breath [29]. A CO_2-Diode Laser Sensor, namely the CO_2-DLS, dedicated to monitor gas-phase

CO_2 in the headspace of champagne glasses was recently developed [22, 30].

In this paper, an upgraded CO_2-DLS aimed at recording an ever increasing amount of data is presented. Upgrading the CO_2-DLS has involved the modification of both data acquisition and data management. Such modifications allowed to map, in space and time and for the very first time, the precise concentration of gas-phase CO_2 in the headspace of a champagne glass.

2. Materials and methods

2.1. Instrument design: a new scanning part

In order to perform the measurement of the gas-phase CO_2 concentration at various points, in the headspace of a champagne glass, for a very short time, the evolution of the CO_2-DLS was required. A schematic representation of the CO_2-DLS with its new part dedicated to the scanning of the headspace of champagne glasses, is presented in Fig. 1.

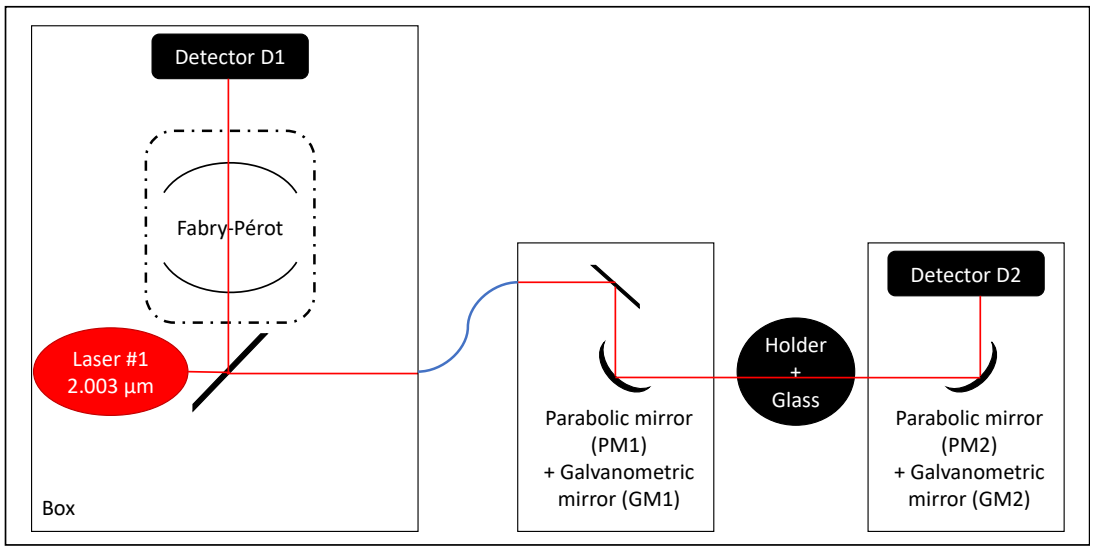

Fig. 1: Schematic representation of the optical set-up.

The optical part, with the laser sources and optical elements for collimation and control, is identical to the one fully described in a precedent work [30]. This set-up is composed by two laser diodes emitting at 2.68 µm (Nanoplus, Germany) and 2.003 µm (EP2004-0-DM, Eblanaphotonics, Ireland), which allow the instrument to cover a wide range of gas-phase CO_2 concentrations. The 2.003 µm laser monitors a weak CO_2 absorption line (R20 line of the $(20^01)_2 \leftarrow (00^00)_1$ band of CO_2, Intensity 1.206×10^{-21} $cm^{-1}/(molec \cdot cm^{-2})$) and allows to measure gas-phase CO_2 between 10% and 100%. The 2.68 µm laser monitors a stronger CO_2 absorption line, allowing the measurement of gas-phase CO_2 below 15%. The present work concerns the technical validation of the CO_2-DLS with a recently developed enological application part dedicated to the scanning of the glass headspace, located on an independent board (3D representation in Fig. 2a). The technical validation has been carried out with the 2.003 µm laser, in order to cover the largest range of gas-phase CO_2 concentrations, between 10 and 100 %.

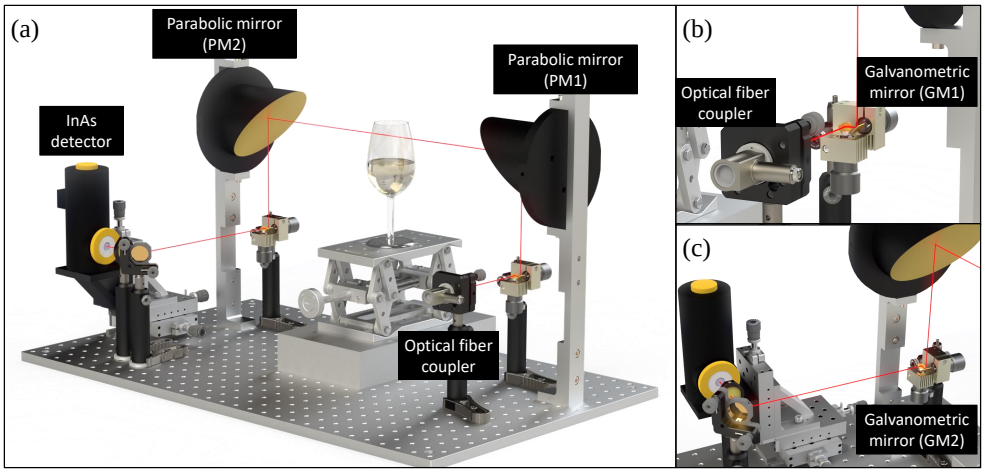

Fig. 2: Global view of the optical set-up created from SolidWorks (Dassault Systèmes, France) (a), with the red line showing the infrared beam, and panels showing both couples of galvanometric mirrors dedicated to the scanning of the glass headspace (b and c).

The scanning part of the CO_2-DLS includes a reflective fiber coupler red (Thorlabs Inc., USA) allowing the connection of the optical fiber, from the optical part of the CO_2-DLS, and the beam collimation (Fig. 2b). A first couple of galvanometric mirrors (GM1, in Fig. 2b model 6210H from Cambridge Technology, USA) is placed at the focus of an off-axis parabolic mirror (PM1) to allow a laser beam translation to a set of (x,y) coordinates of the scanning points in the glass headspace. In this experiment, a $\pm 1.5°$ rotation angle on the first mirror of GM1 allow a ± 1.5 cm beam translation on the horizontal axis (x), a $\pm 1.5°$ rotation angle on the second mirror of GM1 allow a ± 2.25 cm beam translation on the vertical axis (y). PM1 is a 101.6 mm diameter, 152.4 mm focal length off-axis parabolic mirror (model 83976, Edmund Optics, USA). Symmetrically, PM2 and GM2 (same model as PM1 and GM1) allow to balance beam translation in order to detect laser light with a single element cryogenic InAs photodiode (Fig. 2c). A pre-amplifier model DLPCA-200, Femto, Germany) has been added after the cryogenic photodiode (Teledyne Judson Technologies, USA) and the gain has been fixed at 10^6. The use of this new detector, compared to the one used in the previous set-up [30], has improved the signal quality by reducing the noise.

However, it can be noted that the mechanical constraints of the set-up require that the laser beam goes through the focus of only one of the two mirrors of each pair of galvanometric mirrors. The two couples of galvanometric mirrors are controlled each by one external controller, and the motors of the x and y mirrors of each couple are independent. Glasses are placed on a suitable holder (adjustable in height) between the parabolic mirrors. Thus, the laser is reflected in a parallel manner by the off-axis parabolic mirror (PM1) and the laser beam position is moved by GM1 while maintaining the same direction. This device allows to impose a movement on the laser beam and to vary its position horizontally and vertically.With the scanning part, the total optical path (optical part + scanning part of the CO_2-DLS) is extended by 75 cm and the total optical of the 2.003 µm laser path is 175 cm. Thus the absorption by ambient CO_2 (400 ppm) over this distance is less than 1 % and the absorption by the ambient air can be considered as

negligible for the measurements realized by the laser.

2.2. *Upgrading data acquisition and processing*

The instrument is still fully managed using a laboratory made Labview software (National Instruments, USA) driving a NI-7852R FPGA card (National Instruments, USA) used for laser control (temperature set point, waveform generation for laser sweeping, TTL trigger generation and data acquisition) and for the galvanometric mirrors engines control. The FPGA card parameters used for the laser control are summarized in Table 1. The corresponding input current applied to the 2.003 µm laser diode is a 90 mA peak to peak sawtooth signal with an offset of 55 mA. With these parameters, the laser tuning range is centered on the R20 line and is 0.75 cm^{-1} wide. The R20 line FWHM is 0.21 cm^{-1}.

Table 1: Technical characteristics and control parameters of the 2.003 µm laser.

Parameters	2.003 µm Laser @ 2.003 µm
Sample rate (kSamples/s)	1
Loop rate (kHz)	40000
DDS signal frequency (Hz)	42
Signal amplitude ramp (mV)	350
Offset ramp (mV)	350
Signal amplitude TTL (mV)	2500

In this update of the CO_2-DLS, the acquisition of signals is based on the use of a high density digitizer (NI5105) (National Instruments, USA). Five signals are recorded : TTL signal, D1 signal (Fabry-Pérot, noted FP), D2 signal (spectrum), the x mirror position of GM1 and the y mirror position of GM1. The assignment of the full scale input ranges (FSIR) has been adapted in function of each channel, in order to improve the saved data quality. The selection of the different FSIRs is listed in Table 2.

Table 2: Assignment of the channels recorded by the acquisition card and the full scale input ranges assigned to each channel.

Channel	Recorded signal	Full scale input range (V)
0	x mirror position	10
1	y mirror position	10
2	TTL	10
3	D1 signal (FP)	2
4	D2 signal	1

The five channels are recorded with a frequency of 4.10^6 samples/s and a buffer memory system has been set up. All data, previously stored in ASCII format, are now stored in binary format to allow very high speed data transmission and to reduce the size of the generated files. The channels #0 and #1 corresponds to the positions of the mirrors x and y of GM1. The coordinate pair thus refers to a position for the measurement in the glass headspace, that is defined as a pixel. The recorded data thus correspond to a succession of files and each one of them consists of the succession of recorded channels over a regular time interval, i.e. a loop pattern, as in Fig. 3a.

The first step of the pre-treatment consists in rebuilding each channel recorded, as in Fig. 3b. Then, using the channels #0 and #1, the channels #2, #3 and #4 are reconstructed for each position in the glass headspace (i.e. pixel). The useful part of the signals (parts A and B on Fig. 3c) is taken to form a usable data set for each pixel. Finally, the data processing method used to obtain the gas-phase CO_2 concentration is the same as previously described by [30]. Nevertheless, the processing program has been adapted for the new binary format of the data. The measurement of the gas-phase CO_2 concentration is therefore always based on the result of a constrained non-linear fitting. An example of fitting is given in Fig. 4 which corresponds to a non-linear fitting for a spectrum of 50 % of CO_2 mixture obtained with the 2.003 µm laser.

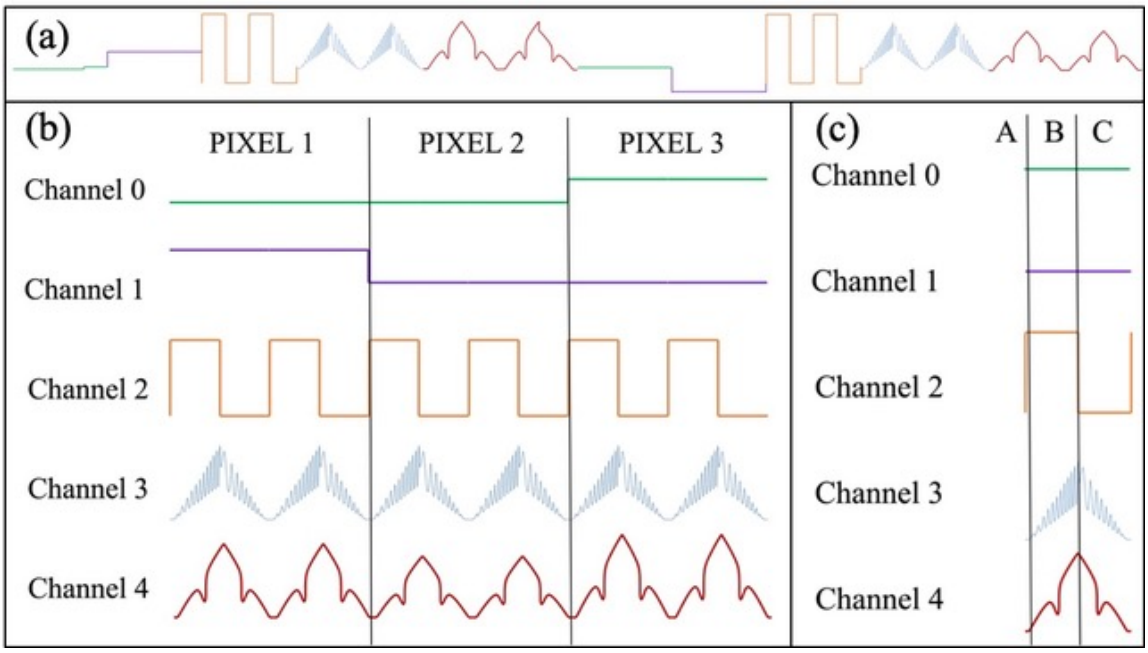

Fig. 3: Schematic representation of the signals, as recorded in the files, corresponding to successive accumulation of the 5 recorded channels (a). Schematic representation of the data recorded during the scanning of three pixels, with the position of the mirror x (Galvanometric Mirror GM1) in green on channel #0, the position of the mirror y (Galvanometric Mirror GM1) in purple on channel #1, the TTL signal in yellow on channel #2, the signal recorded by the detector D1 (Fabry-Pérot) in blue on channel #3 and the signal recorded by the detector D2 (spectra) in red on channel #4 (b). Zoom of the signals recorded during the scanning of a single pixel, in A the part below the laser threshold, in B the part used for the estimation of the intensity baseline (I_0) and for the transmitted intensity (I) and in C the part corresponding to the return of the laser at the initial frequency (decreasing part of the triangular laser control signal) (c).

2.3. *Measurements of standard gas-phase CO_2 samples*

A technical validation of the CO_2-DLS, with its new part dedicated to the scanning of the headspace of a champagne glass, has been carried out. It has been highlighted, in a previous study [22], that during the pouring step, the gas-phase CO_2 concentration measured is in a large range, between 10 % and 100 %. Moreover, the aim of this upgraded device is to measure the gas-phase CO_2 concentration in the whole headspace of champagne

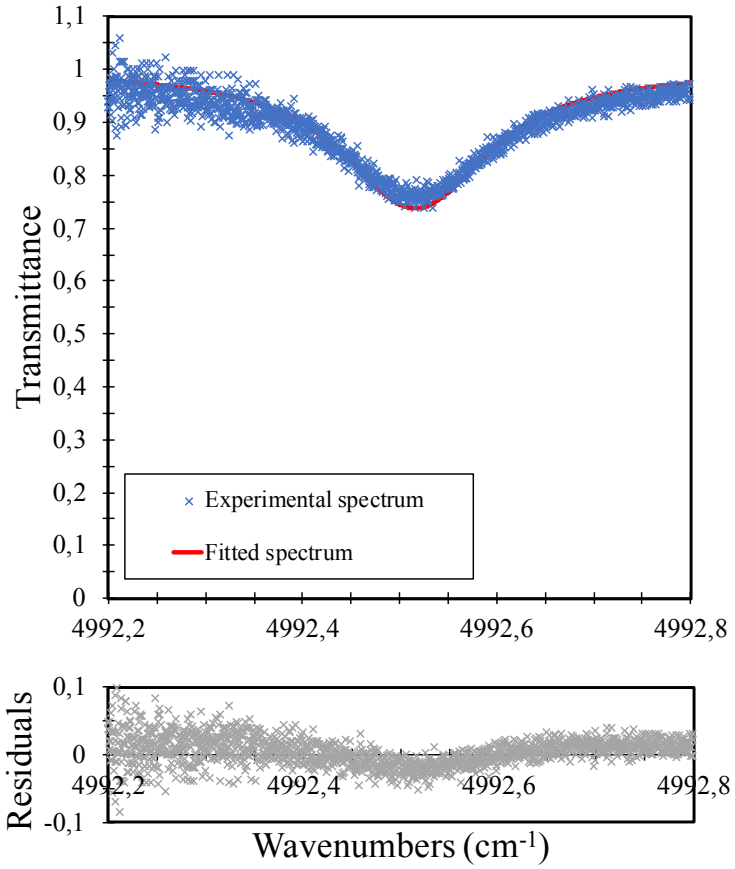

Fig. 4: Constrained non-linear fitting of a spectrum obtained with the laser emitting at 2.003 µm, of a 50 % concentration of gas-phase CO_2.

glasses including close to the liquid surface, and it can be expected that the measured concentrations near the liquid surface even reach 100 %. This is why the technical validation has been done only with the 2.003 µm laser.

Various dry air/CO_2 gas mixtures were prepared through a mass flow dilutor (Alytech GasMix), with increasing CO_2 concentrations ranging from 10 to 100 % (and with concentration errors varying between 0.001 % and 0.4 %, respectively). A gas cell analysis was

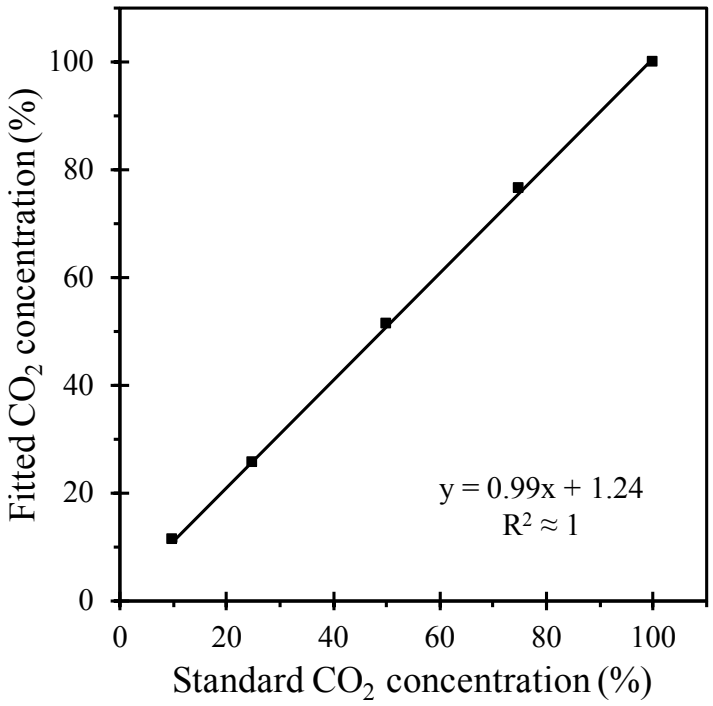

Fig. 5: Concentrations of gas-phase CO_2 as determined through the CO_2-DLS, fitted as a function of the dry air/CO_2 gas mixtures standards.

designed from an INAO glass and filled with the various dry air/CO_2 gas mixtures at a pressure of 1 bar (absolute) (see Appendix A and Fig.A.10). The baseline was recorded with the empty cell. Then, a hundred spectra were recorded for each tested CO_2 concentration. Finally, the results are displayed in Fig. 5, and fitted linearly with the concentration of standards in the whole range of CO_2 concentration varying between 10 % and 100 %. The slope of the regression line being equal to 0.99, the upgraded CO_2-DLS (with its new part dedicated to the scanning) therefore allowed to perfectly retrieve the standard CO_2 concentration with a very good agreement (in the range between 10 and 100 %).

2.4. Samples and enological application protocol

2.4.1. Champagne samples

A commercial Champagne wine, in standard 75 cL bottles with a blend of Chardonnay, Pinot Noir and Pinot Meunier base wines (champagne Nicolas Feuillatte, 12.5 %vol.) has been used. Since their elaboration, bottles were stored in a cool cellar at 12 °C and the champagne was poured at 12 °C. It was found to hold $(9.40 \pm 0.05)\,\mathrm{g \cdot L^{-1}}$ of dissolved CO_2 before pouring, by using the analytical method described in [4].

2.4.2. The glasses used and their washing protocol

A machine-blown glass, called Absolu glass (Lehmann glass, Marne, France), was used for this set of experiments. It is a hybrid glass, curved inwards at the top, with a total volume of 380 mL and with a global shape similar to the one of a still wine glass. When filled with 100 mL of champagne, the headspace is of 280 mL is still large. This is why it has been chosen in order to study the gas-phase CO_2 distribution above champagne. A 3D scheme of the Absolu glass is presented in Fig. 6a. Moreover, the set of glasses were laser-etched champagne glasses, in order to promote standardized conditions of effervescence (i.e., a rate of bubbling accurately controlled through laser beam-driven bubble nucleation sites). To promote bubble formation, such glasses were simply etched on their bottom, with several laser beam impacts. A sudden cooling after the laser beam impact causes a network of crevices at the glass surface, as seen in the micrographs of adjoining laser beam impacts displayed in Fig. 6b-d. As champagne is served in such laser-etched glasses, this network of tiny crevices at the bottom of the glass surface enables the entrapment of tiny air pockets. For a global overview of how laser-etched champagne glasses promote bubble formation, see [1], and references therein. Finally, before each experiment, the glasses were thoroughly washed using the protocol described in [22]. Thus, effervescence is strictly restricted to the six artificial bubble nucleation sites, at the bottom of the glass.

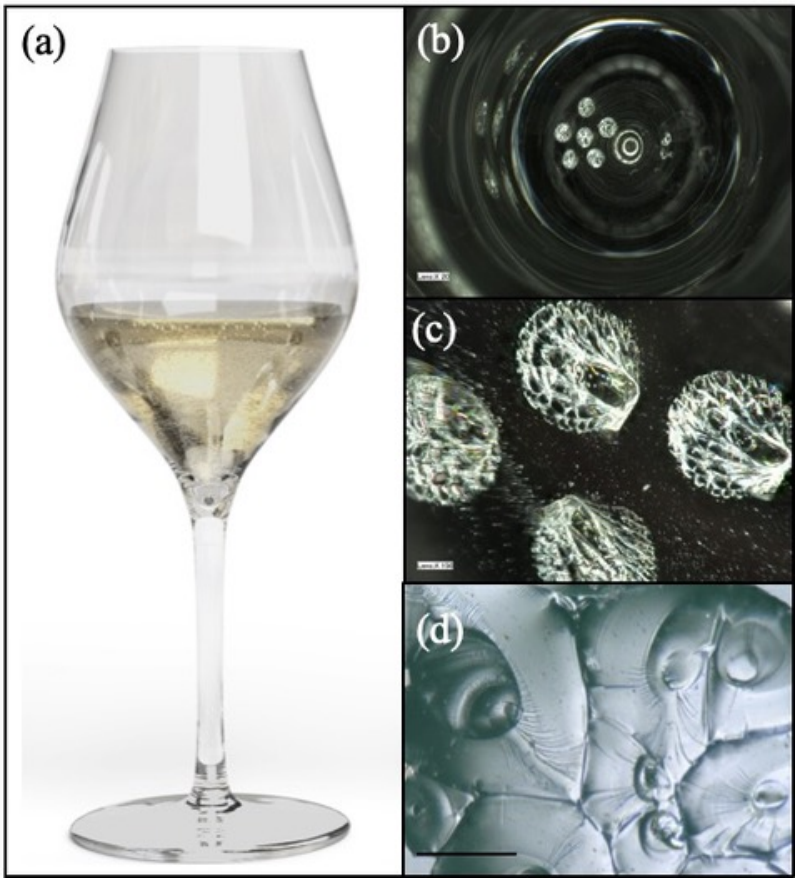

Fig. 6: Scheme (created from SolidWorks) of the Absolu glass filled with 100 mL of champagne (a). Micrographs of the six laser beam impacts found at the bottom of the laser-etched Absolu glass (b and c), one of them being enlarged in (d) and showing a network of crevices with characteristic open apertures close to 2 µm (bar = 100 µm).

2.4.3. *Definition of the pixels in the glass headspace*

In order to study the whole headspace of the glass, 100 mL of champagne at 12 °C were poured and nine pixels were defined (Fig. 7a) on three different levels vertically, i.e. levels A, B and C, and three different locations horizontally, including three pixels along the axis of symmetry of the glass (i.e. #2) and three at 1.5 cm of the symmetry axis on each side, i.e. #1 and #3. In Table 3, the distances between the pixels and the glass edge and the liquid surface (100 mL), as well as the lengths of the optical path are given. As it can be seen in Table 3, the path lengths for two pixels at the same measurement level on each side of the symmetry axis, i.e. #1 and #3, is different because a slight deviation of the laser beam was observed.

It can be noted that the minimum distance between the liquid surface and the measurement level has been fixed at 2 cm. This distance between the wine surface and the laser beam path has been chosen in order to limit a possible source of trouble for the measurement caused by champagne aerosol droplets formed in the first ten seconds following the beginning of the pouring.

In order to more deeply decipher the gas-phase CO_2 distribution above the champagne surface, five pixels vertically arranged along the axis of symmetry of the glass were defined in the glass headspace, as shown in Fig. 7b. The five pixels are located between 1 cm below the glass edge (A2), and 2 cm above the champagne surface (C2). The relevant geometrical parameters are presented in Table 4.

The two sets of experiments were performed in a thermo-regulated room (20 ± 1 °C). The Absolu glass, was previously level-marked with 100 mL of distilled water, and placed on its suitable holder. In order to limit the formation of foam and the presence of a liquid film on the glass wall, 100 mL of champagne (at 12 °C) were poured carefully in the glass. The pouring process lasts approximately 10-15 s. Actually, the presence of foam or a liquid film on the glass wall may reduce or even stop the signal. The monitoring of gas-phase CO_2 concentration begins 30 s before the beginning of the pouring process in order to

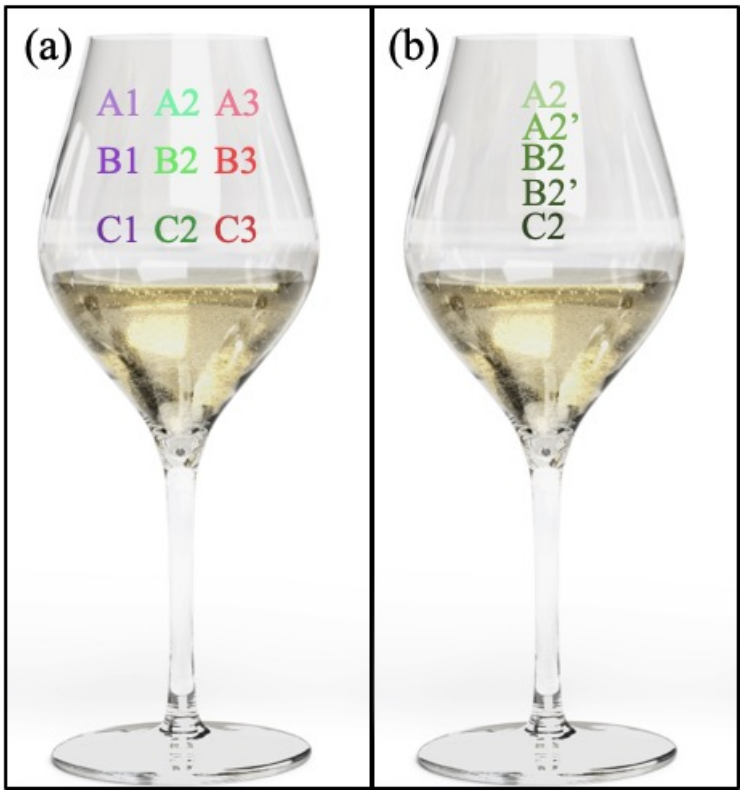

Fig. 7: Schemes (created from SolidWorks) of the Absolu glass filled with 100 mL of champagne, showing the respective location of the nine (a) and five pixels (b) dedicated to the simultaneous measurements of gas-phase CO_2 in the glass headspace.

record experimental baselines for each pixel while the glass is filled with ambient air. The contribution of ambient CO_2 (400-1000 ppm in the lab) is considered to be negligible compared to that of CO_2 degassed by the liquid ($\geq 10\,\%$) Four successive pourings from two distinct bottles have been carried out then averaged for each experiment.

Table 3: Location and optical path length of the nine pixel, as defined in Fig. 7a, for the simultaneous measurement of gas-phase CO_2 in the headspace of the Absolu glass.

Pixels	Distance between the pixel and the liquid surface (cm)	Distance between the pixel and the edge of the glass (cm)	Optical path length (cm)
A1	6.5	1	4.8
B1	4.5	3	6.1
C1	2	5.5	7.3
A2	6.5	1	5.7
B2	4.5	3	6.7
C2	2	5.5	8
A3	6.5	1	5
B3	4.5	3	6.3
C3	2	5.5	7.6

Table 4: Location and optical path length of the five pixels vertically arranged along the axis of symmetry, as defined in Fig. 7b, for the simultaneous measurement of gas-phase CO_2 in the headspace of the Absolu glass.

Pixels	Distance between the pixel and the liquid surface (cm)	Distance between the pixel and the edge of the glass (cm)	Optical path length (cm)
A2	6.5	1	5.7
A2′	5.5	2	6.4
B2	4.5	3	6.7
B2′	3.5	4	7.5
C2	2	5.5	8

3. Results and discussion

3.1. Gas-phase CO_2 concentration measurement at nine different pixels in the glass headspace

During the pouring step, and within the five next minutes following pouring, the time dependence of the gas-phase CO_2 concentration was simultaneously measured at nine different pixels found in the glass headspace, as shown in the graph displayed in Fig. 8. Regardless of the pixel at which gas-phase CO_2 measurement is performed, the global shape described by the real-time monitoring of gas-phase CO_2 concentration is identical to what was underscored in previous works [22, 30]. In the first stage of the monitoring, a rapid growth of gas-phase CO_2 concentration is systematically observed, until a maximum is reached only several seconds after the end of the pouring step. This rapid growth of gas-phase CO_2 in the glass headspace during the pouring step is interpreted in light of the huge losses of dissolved CO_2 unveiled during this stage. Actually, the turbulences of the pouring step lead to the loss of several grams per liter of CO_2 from the liquid phase supersaturated with dissolved CO_2 [5, 31, 32]. In a second step, a global decrease of gas-phase CO_2 concentrations found in the headspace of the glass is observed. Interestingly, a similar evolution of gas-phase CO_2 concentrations was measured by a CO_2 gas sensor above beer glasses at concentrations below 1 % [20].

Moreover, as it can be seen in Fig. 8, the three different vertical levels of measurement (i.e., A, B and C) clearly differ quantitatively from each other in terms of gas-phase CO_2 concentrations. The maximum concentration reached several seconds after the end of pouring process is about 17 % at 6.5 cm above the liquid surface (pixels A1, A2 and A3), against 32 % at 4.5 cm above the liquid surface (pixels B1, B2 and B3) and close to 50 % at 2 cm above the liquid surface (pixels C1, C2 and C3). Therefore, the closer one is to the champagne surface, the higher the concentration of gas-phase CO_2 after the pouring step. It is worth noting that this trend can be observed during the global decrease in gas-phase CO_2 observed within the five next minutes following the pouring, as shown in Fig. 8.

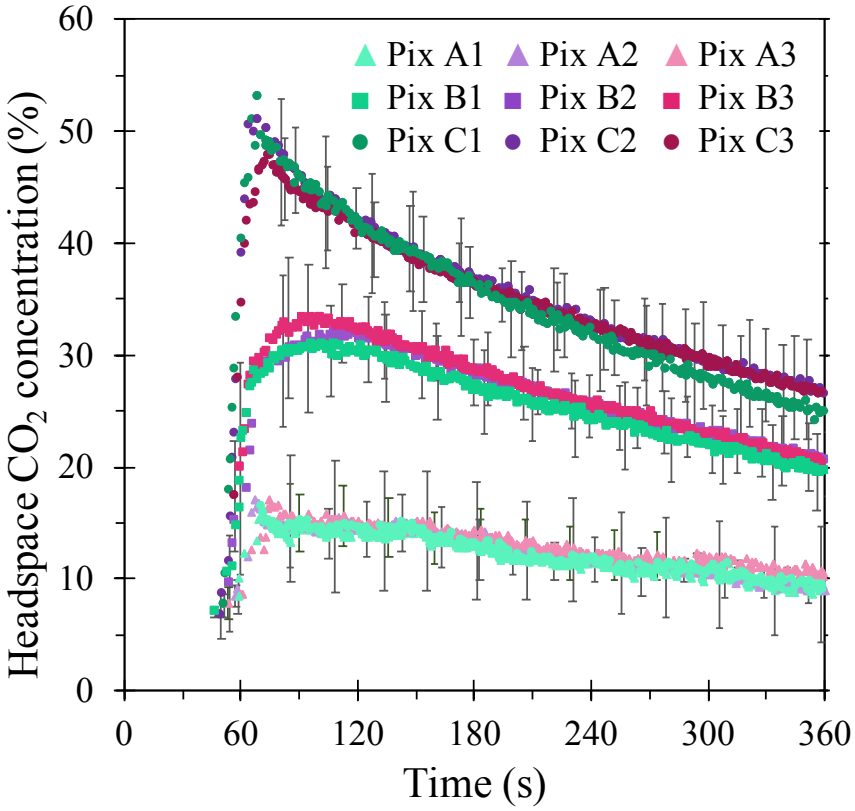

Fig. 8: Simultaneous measurements, as time elapses, of gas-phase CO_2 concentrations (in %) found at the nine pixels located in the headspace of the glass, as defined in Fig. 7a. The dots correspond to pixels C1, C2 and C3, the squares to pixels B1, B2 and B3, and the triangles to pixels A1, A2 and A3. The data resulting from four successive pouring were averaged. Error bars indicating standard deviation (n=4 except for A2, A3 and C1 n=3) were added to every 1/20 time point of the CO_2-DLS data. The acquisition data frequency is equal to 42 Hz.

This set of data therefore allows to conclude that a strong vertical gradient of gas-phase CO_2 quickly forms in the headspace of the glass, as soon as the pouring step is achieved. This vertical gradient persists during the five next minutes following the pouring process. Nevertheless, it is also noteworthy to mention that the gas-phase CO_2 concentrations found in the glass headspace are very similar at the same horizontal level of measurement (during the pouring step, and within the five next minutes of monitoring). The CO_2-DLS therefore unambiguously unveiled horizontal homogeneity in the glass headspace, in terms of gas-phase CO_2 concentrations.

3.2. Close-up on the vertical gradient, along the symmetry axis of the glass headpsace

In order to better decipher the vertical stratification of gas-phase CO_2 in the glass headspace, another set of data has been performed. During the pouring step and within the five next minutes, real-time monitoring of gas-phase CO_2 was performed in the headspace of the same glass, at five vertically arranged pixels (defined in Fig. 7b). Results are shown in Fig. 9. Firstly, the time dependent gas-phase CO_2 concentrations clearly differ from one pixel to another, thus unambiguously confirming the vertical gradient of gas-phase CO_2 unveiled through the CO_2-DLS. Secondly, it is worth noting that the averaged gas-phase CO_2 concentrations measured in this experiment are slightly lower than those previously retrieved and shown in Fig. 8. Actually, the manual pouring of champagne in the glass leads to a lack of reproducibility and thus sometimes to slight differences between distinct series of measurements, even under the same tasting conditions, with the same champagne samples.

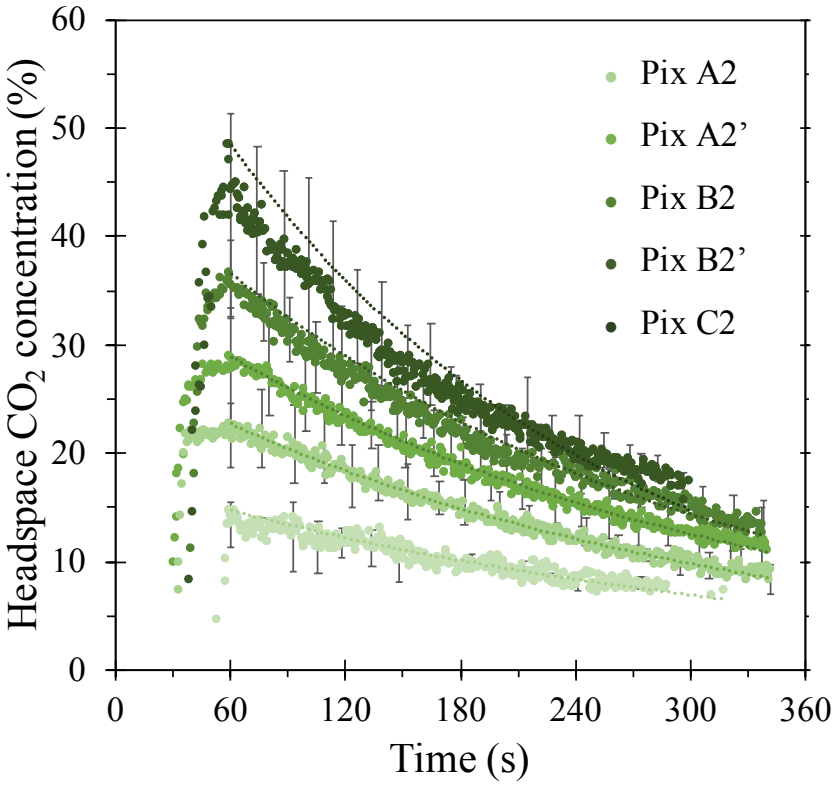

Fig. 9: Simultaneous measurements, as time elapses, of gas-phase CO_2 concentrations (in %) found at the five pixels vertically arranged along the axis of symmetry of the glass headspace, as defined in Fig. 7b. The data resulting from four successive pouring were averaged. Error bars indicating standard deviation (n=4 except for A2, A3 and C1 n=3) were added to every 1/20 time point of the CO_2-DLS data. The acquisition data frequency is equal to 42 Hz.

Moreover, and regardless the level at which the measurement is performed along the axis of symmetry of the glass headspace, the temporal decrease of the gas-phase CO_2 concentration following the rapid growth observed during the pouring step (presented in Fig. 9) follows an exponential decay-type model described hereafter:

$$[CO_2](t) \approx [CO_2]_M \exp\left(-\frac{t}{\tau}\right) \quad (1)$$

with $[CO_2]_M$ being the maximum average gas-phase CO_2 concentration reached several seconds after the pouring step (in %), t being the time (in s), and τ being the timescale of the exponential decay-type model (in s).

Table 5: Parameters of the exponential decay-type model fitting the temporal decrease of the average gas-phase CO_2 concentrations for the five pixels vertically arranged along the axis of symmetry of the glass headspace.

Pixel	$[CO_2]_M$ (%)	τ (s)	R^2
A2	14.5	312	0.92
A2′	22.5	282	0.99
B2	28.7	285	0.99
B2′	36.3	254	0.98
C2	48.1	200	0.98

Table 5 compiles the various parameters of the exponential decay-type model, for the five various pixels vertically arranged along the axis of symmetry of the glass headspace. This second set of data unambiguously confirms the formation of a strong vertical gradient of gas-phase CO_2 in the glass headspace at the end of the pouring step, with decreasing CO_2 concentrations while moving away from the champagne surface. This vertical gradient of gas-phase CO_2 persists during the five next minutes following pouring, but with ever decreasing CO_2 concentrations as time elapses. This vertical stratification of CO_2 betrays the fact that the density of gas-phase CO_2 ($\rho_{CO_2} \approx 1.8\,g \cdot L^{-1}$ at 20 °C) is approximately

1.5 times higher than the density of dry air ($\rho_{air} \approx 1.2\,g \cdot L^{-1}$ at 20 °C). The cloud of gas-phase CO_2 escaping from champagne during the pouring step and within the five next minutes therefore tends to naturally stagnate and sediment above the champagne surface, as already observed by [33] through infrared imaging.

4. Conclusion

Key upgrades to a previously developed CO_2-Diode Laser Sensor (CO_2-DLS) resulted in an instrument well designed for accurate, simultaneous, and high-frequency measurements of gas-phase CO_2 concentrations in the whole headspace of glasses poured with champagne. Immediately after starting to dispense champagne into a glass, and within the five next minutes following, real-time monitoring of gas-phase CO_2 was conducted at different locations in the headspace of the glass, with a 24 ms time resolution. Immediately after the pouring step, the CO_2-DLS highlighted a strong vertical gradient of gas-phase CO_2 above the champagne surface, thus unveiling a vertical stratification of gas-phase CO_2 in the headspace of the glass (with decreasing CO_2 concentrations while moving away from the champagne surface, and as time elapses). Moreover, the sets of data unambiguously unveiled horizontal homogeneity in the glass headspace in terms of gas-phase CO_2 concentrations. In a near future, this upgraded CO_2-DLS will enable to further explore the impact of various champagne tasting parameters on the gas-phase CO_2 concentrations found in the headspace inhaled by champagne tasters, such as the tasting glass shape, the champagne temperature, or the volume dispensed for example.

Acknowledgements

Thanks are due to the Association Recherche Oenologie Champagne Université for financial support and to Champagne Nicolas Feuillate for supplying us with various champagne samples and glasses. The authors also thank Florian Lecasse and Nicolas Chauvin for their technical help.

References

[1] G. Liger-Belair, Effervescence in champagne and sparkling wines: From grape harvest to bubble rise, The European Physical Journal Special Topics 226 (1) (2017) 3–116. doi:10.1140/epjst/e2017-02678-7.

[2] G. Liger-Belair, D. Carvajal-Perez, C. Cilindre, J. Facque, M. Brevot, F. Litoux-Desrues, V. Chaperon, R. Geoffroy, Evidence for moderate losses of dissolved CO_2 during aging on lees of a champagne prestige cuvee, Journal of Food Engineering 233 (2018) 40–48. doi:10.1016/j.jfoodeng.2018.03.026.

[3] L. Hewson, T. Hollowood, S. Chandra, J. Hort, Gustatory, olfactory and trigeminal interactions in a model carbonated beverage, Chemosensory Perception 2 (2009) 94–107. doi:10.1007/s12078-009-9043-7.

[4] G. Liger-Belair, S. Villaume, C. Cilindre, G. Polidori, P. Jeandet, CO_2 Volume fluxes outgassing from champagne glasses in tasting conditions: Flute versus coupe, Journal of Agricultural and Food Chemistry 57 (11) (2009) 4939–4947. doi:10.1021/jf900804j.

[5] G. Liger-Belair, A. Conreux, S. Villaume, C. Cilindre, Monitoring the losses of dissolved carbon dioxide from laser-etched champagne glasses, Food Research International 54 (1) (2013) 516–522. doi:10.1016/j.foodres.2013.07.048.

[6] F. Beaumont, G. Liger-Belair, Y. Bailly, G. Polidori, A synchronized particle image velocimetry and infrared thermography technique applied to convective mass transfer in champagne glasses, Experiments in Fluids 57 (5) (2016) 85. doi:10.1007/s00348-016-2180-2.

[7] F. Beaumont, G. Liger-Belair, G. Polidori, Unveiling self-organized two-dimensional (2D) convective cells in champagne glasses, Journal of Food Engineering 188 (2016) 58–65. doi:10.1016/j.jfoodeng.2016.05.012.

[8] G. Liger-Belair, S. Villaume, C. Cilindre, P. Jeandet, Kinetics of CO_2 fluxes outgassing from champagne glasses in tasting conditions : The role of temperature, Journal of Agricultural and Food Chemistry 57 (5) (2009) 1997–2003.

[9] C. Spence, X. Wan, Beverage perception and consumption: The influence of the container on the perception of the contents, Food Quality and Preference 39 (2015) 131–140. doi:10.1016/j.foodqual.2014.07.007.

[10] E. E. Southwick, R. F. Moritz, Social control of air ventilation in colonies of honey bees, Apis mellifera, Journal of Insect Physiology 33 (9) (1987) 623–626. doi:10.1016/0022-1910(87)90130-2.

[11] S. Hanstein, D. De Beer, H. H. Felle, Miniaturised carbon dioxide sensor designed for measurements within plant leaves, Sensors and Actuators, B: Chemical 81 (1) (2001) 107–114. doi:10.1016/S0925-4005(01)00939-X.

[12] H. J. Schellnhuber, 'Earth system' analysis and the second Copernican revolution, Nature 402 (6761 SUPPL. 1) (1999) 19–23. doi:10.1038/35011515.

[13] C. L. Sabine, R. A. Feely, N. Gruber, R. M. Key, K. Lee, J. L. Bullister, R. Wanninkhof, C. S. Wong, D. W. R. Wallace, B. Tilbrook, F. J. Millero, T.-H. Peng, A. Kozyr, T. Ono, A. F. Rios, The oceanic sink for anthropogenic CO_2, Science 305 (5682) (2004) 367–371. doi:10.1126/science.1097403.

[14] J. N. Carleton, A. M. Donoghue, W. K. Porter, Mechanical model testing of rebreathing potential in infant bedding materials, Archives of Disease in Childhood 78 (4) (1998) 323–328. doi:10.1136/adc.78.4.323.

[15] J. Zosel, W. Oelßner, M. Decker, G. Gerlach, U. Guth, The measurement of dissolved and gaseous carbon dioxide concentration, Measurement Science and Technology 22 (2011) 1–45. doi:10.1088/0957-0233/22/7/072001.

[16] C. Gonzalez Viejo, D. D. Torrico, F. R. Dunshea, S. Fuentes, Bubbles, foam formation, stability and consumer perception of carbonated drinks: A review of current, new and emerging technologies for rapid assessment and control, Foods 8 (12) (2019) 596. doi:10.3390/foods8120596.

[17] P. Puligundla, J. Jung, S. Ko, Carbon dioxide sensors for intelligent food packaging applications, Food control 25 (1) (2012) 328–333. doi:10.1016/j.foodcont.2011.10.043.

[18] E. Robert, C. Klein, Improved method for CO_2 measurements, Brewing and Beverage Industry International 5 (2007) 32–35.

[19] C. Gonzalez Viejo, S. Fuentes, A. Godbole, B. Widdicombe, R. R. Unnithan, Development of a low-cost e-nose to assess aroma profiles: An artificial intelligence application to assess beer quality, Sensors and Actuators, B: Chemical 308 (2020) 127688. doi:10.1016/j.snb.2020.127688.

[20] C. Gonzalez Viejo, S. Fuentes, G. Li, R. Collmann, B. Condé, D. Torrico, Development of a robotic pourer constructed with ubiquitous materials, open hardware and sensors to assess beer foam quality using computer vision and pattern recognition algorithms: RoboBEER, Food Research International 89 (2016) 504–513. doi:10.1016/j.foodres.2016.08.045.

[21] C. Cilindre, A. Conreux, G. Liger-Belair, Simultaneous monitoring of gaseous CO_2 and ethanol above champagne glasses via micro-gas chromatography (μGC), Journal of Agricultural and Food Chemistry 59 (13) (2011) 7317–7323. doi:10.1021/jf200748t.

[22] A.-L. Moriaux, R. Vallon, B. Parvitte, V. Zeninari, G. Liger-belair, C. Cilindre, Monitoring gas-phase CO_2 in the headspace of champagne glasses through combined diode laser spectrometry and micro-gas chromatography analysis, Food Chemistry 264 (January) (2018) 255–262. doi:10.1016/j.foodchem.2018.04.094.

[23] G. M. Gibson, B. Sun, M. P. Edgar, D. B. Phillips, N. Hempler, G. T. Maker, G. P. A. Malcolm, M. J. Padgett, Real-time imaging of methane gas leaks using a single-pixel camera, Optics Express 25 (4) (2017) 2998–3005. arXiv:1607.08236, doi:10.1126/sciadv.1601782.

[24] R. F. Curl, F. K. Tittel, Tunable infrared laser spectroscopy, Annual Reports Section "C" (Physical Chemistry) 98 (2002) 219–272. doi:10.1039/B111194A.

[25] V. Zéninari, A. Vicet, B. Parvitte, L. Joly, G. Durry, In situ sensing of atmospheric CO_2 with laser diodes near 2.05 μm: A spectroscopic study, Infrared Physics and Technology 45 (3) (2004) 229–237. doi:10.1016/j.infrared.2003.11.004.

[26] G. Durry, J. S. Li, I. Vinogradov, A. Titov, L. Joly, J. Cousin, T. Decarpenterie, N. Amarouche, X. Liu, B. Parvitte, O. Korablev, M. Gerasimov, V. Zéninari, Near infrared diode laser spectroscopy of C_2H_2, H_2O, CO_2 and their isotopologues and the application to TDLAS, a tunable diode laser spectrometer for the martian PHOBOS-GRUNT space mission, Applied Physics B: Lasers and Optics 99 (1-2) (2010) 339–351. doi:10.1007/s00340-010-3924-y.

[27] X. Zhu, S. Yao, W. Ren, Z. Lu, Z. Li, TDLAS monitoring of carbon dioxide with temperature compensation in power plant exhausts, Applied Sciences (Switzerland) 9 (3) (2019) 1–15. doi:10.3390/app9030442.

[28] J. Chen, C. Li, M. Zhou, J. Liu, R. Kan, Z. Xu, Measurement of CO_2 concentration at high-temperature based on tunable diode laser absorption spectroscopy, Infrared Physics and Technology 80 (2017) 131–137. doi:10.1016/j.infrared.2016.11.016.

[29] C. Wang, P. Sahay, Breath analysis using laser spectroscopic techniques: Breath biomarkers, spectral fingerprints, and detection limits, Sensors 9 (10) (2009) 8230–8262. doi:10.3390/s91008230.

[30] A.-L. Moriaux, R. Vallon, C. Cilindre, B. Parvitte, G. Liger-Belair, V. Zeninari, Development and validation of a diode laser sensor for gas-phase CO_2 monitoring above champagne and sparkling wines, Sensors and Actuators B: Chemical 257 (2018) 745–752. doi:10.1016/j.snb.2017.10.165.

[31] G. Liger-Belair, M. Bourget, S. Villaume, P. Jeandet, H. Pron, G. Polidori, On the Losses of Dissolved CO_2 during Champagne Serving, Journal of Agricultural and Food Chemistry 58 (15) (2010) 8768–8775. doi:10.1021/jf101239w.

[32] G. Liger-Belair, M. Parmentier, C. Cilindre, More on the losses of dissolved CO_2 during champagne serving: Toward a multiparameter modeling, Journal of Agricultural and Food Chemistry 60 (47) (2012) 11777–11786. doi:10.1021/jf303574m.

[33] G. Liger-Belair, G. Polidori, V. Zéninari, Unraveling the evolving nature of gaseous and dissolved carbon dioxide in champagne wines: A state-of-the-art review, from the bottle to the tasting glass, Analytica Chimica Acta 732 (2012) 1–15. doi:10.1016/j.aca.2011.10.007.

Appendix A. INAO Glass

The term INAO means "Institut National des Appellations d'Origine". The INAO glass is a certified tasting glass with a total volume capacity of 21 cL. Indeed, this tasting glass meets the requirements of the French (NF V09-110 June 1971) and International (ISO 3591:1977) standards regarding its physical and dimensional characteristics. The INAO is widely used for still wines and sparkling wines tasting, by both professionals and consumers. A photograph of the gas cell designed with an INAO glass is presented in Fig A.10.

Fig. A.10: Photograph of the gas cell designed with an INAO glass